Muon g-2 and/or B anomalies in some gauge extensions of SM

Pyungwon Ko (KIAS)

Muon Anomalies Workshop (MAW)
Hoam SNU, May 21 (Fri), 2021

Contents

- Muon g-2 and B anomalies : talks by exp colleagues
- $U(1)_{L_\mu - L_\tau}$ models
- Other U(1) models
- $R(D^{(*)})$ vs Top FCNC
- Conclusion
- NB : SUSY, 2(3)HDM scenarios : not covered in this talk

Muon g-2

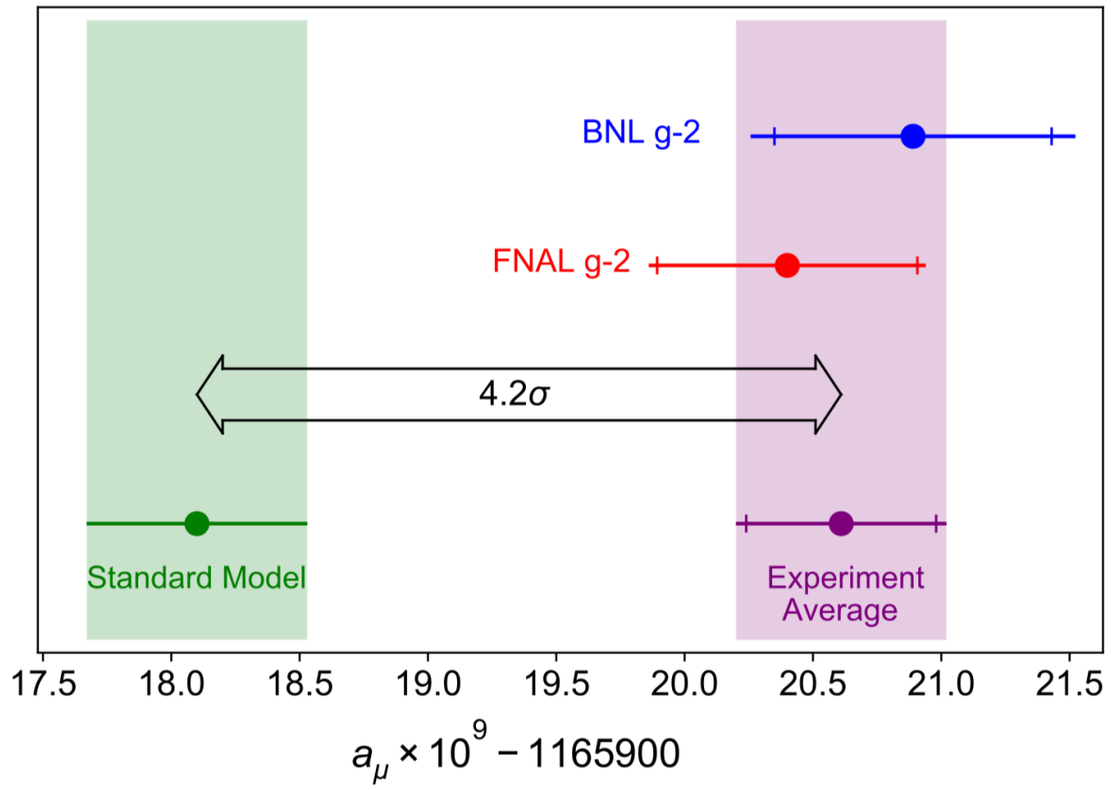

The Muon g-2 Collaboration, 2104.03281

Excellent example for graduate students

- **Relativistic E&M (spinning particle in EM fields)**
- **Special relativity (time dilation)**
- **(V-A) structure of charged weak interaction**

B anomalies

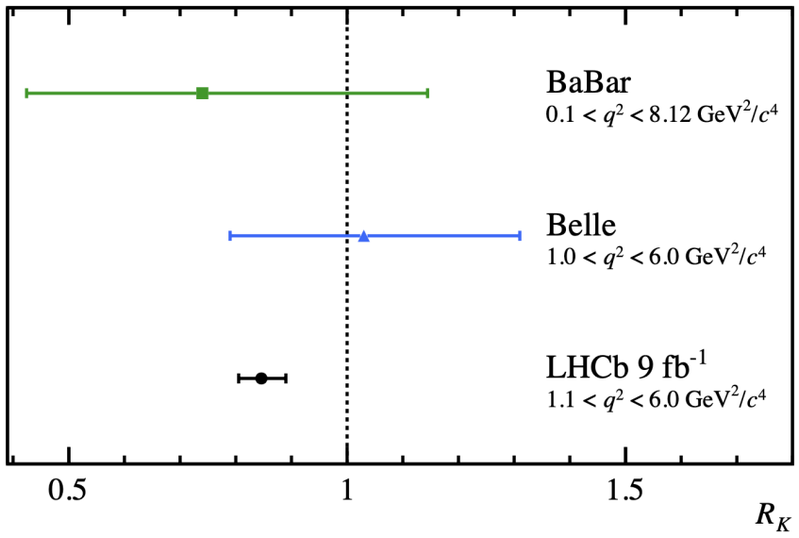

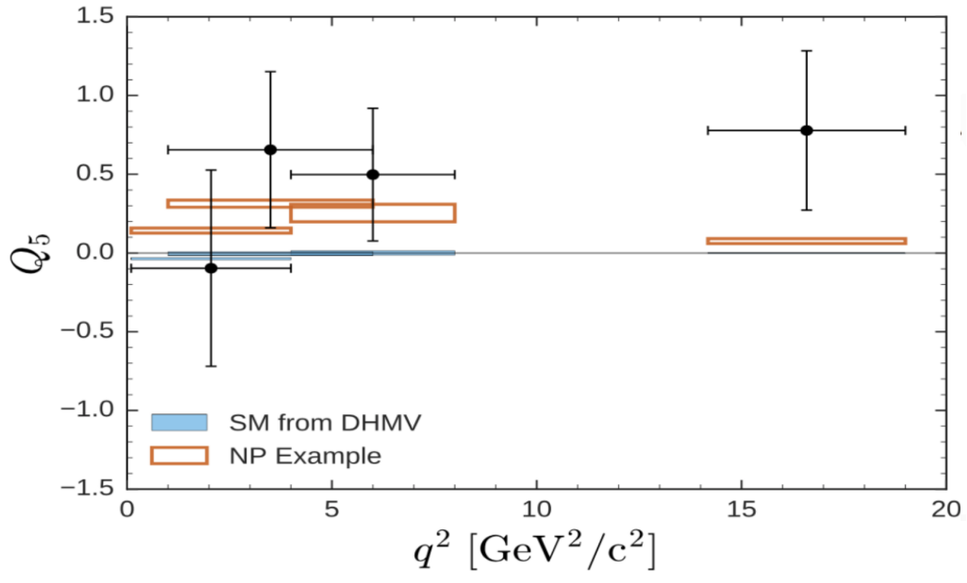

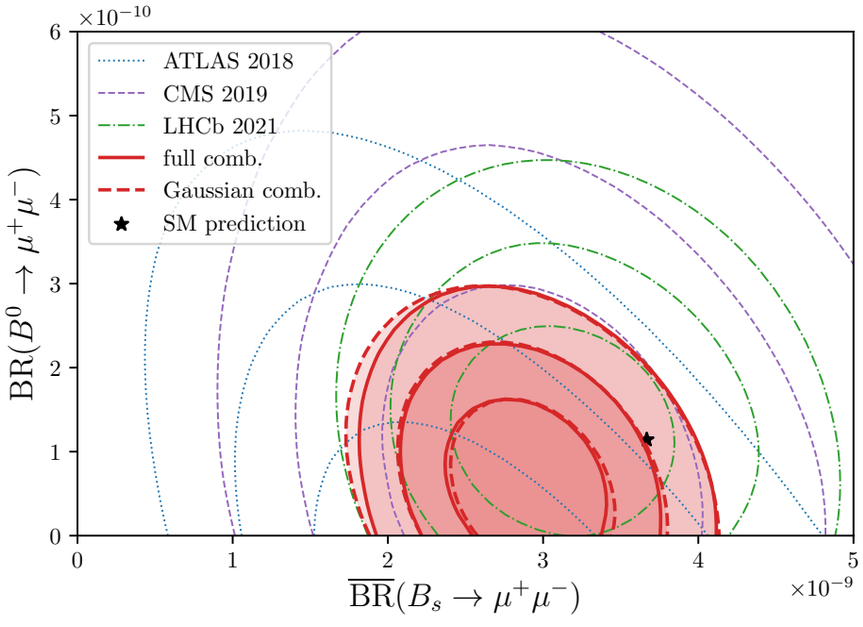

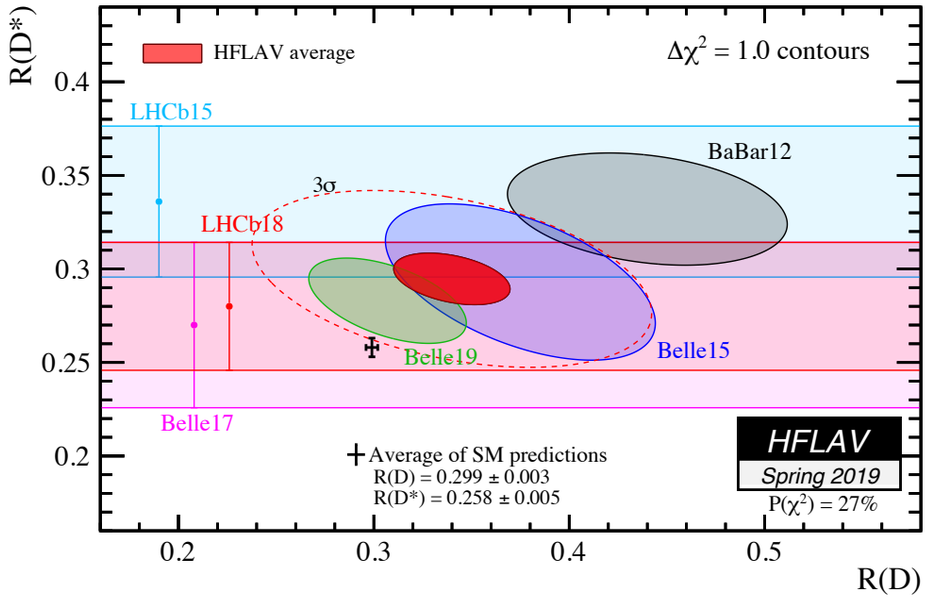

HFLAV, hflav.web.cern.ch

Model indep. analysis

Before Moriond 2021

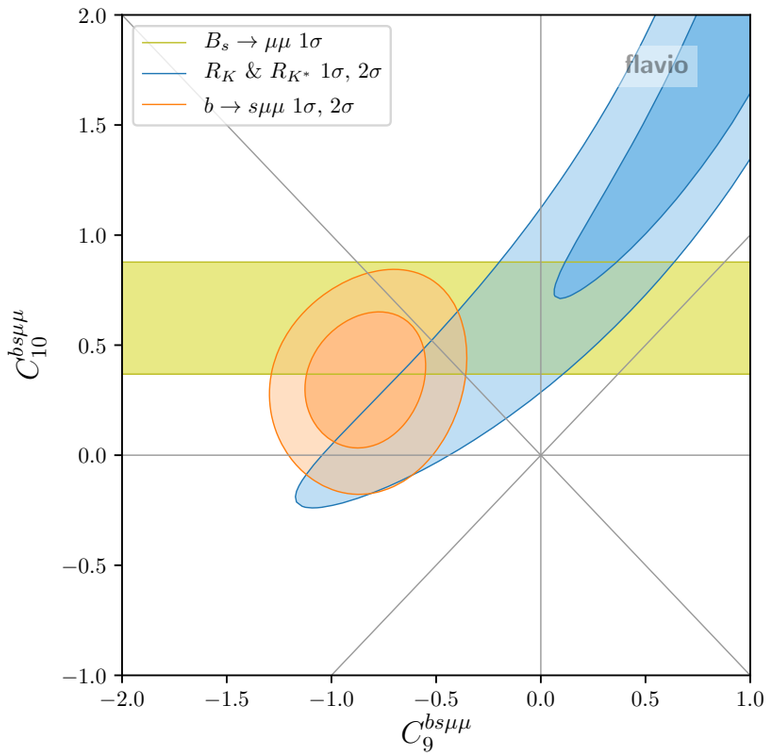

After Moriond 2021

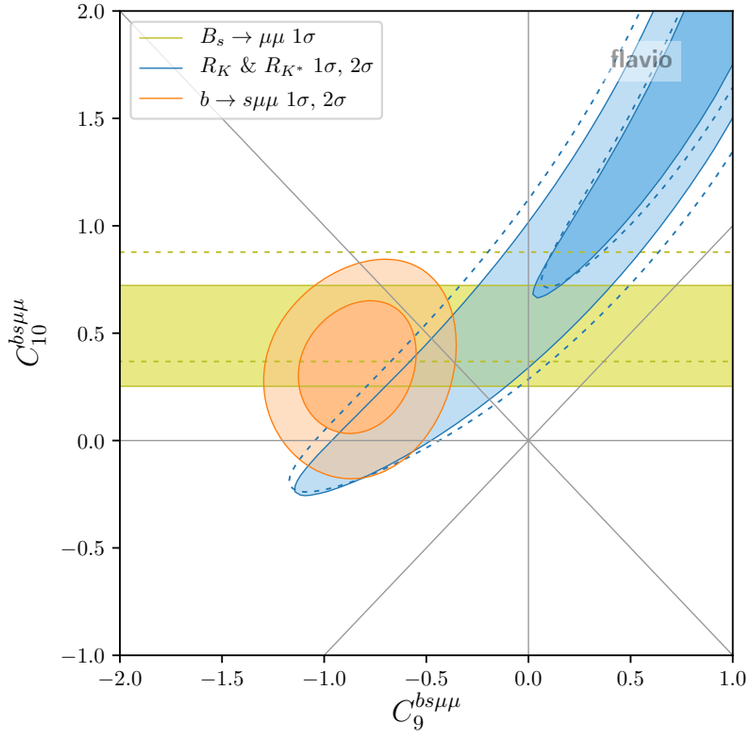

After Moriond 2021

- R_K **: smaller uncertainty**
- $B_s \to \mu\mu$ **: smaller uncertainty &**

better agreement with $b \to s\mu\mu$

Model indep. analysis

Before Moriond 2021

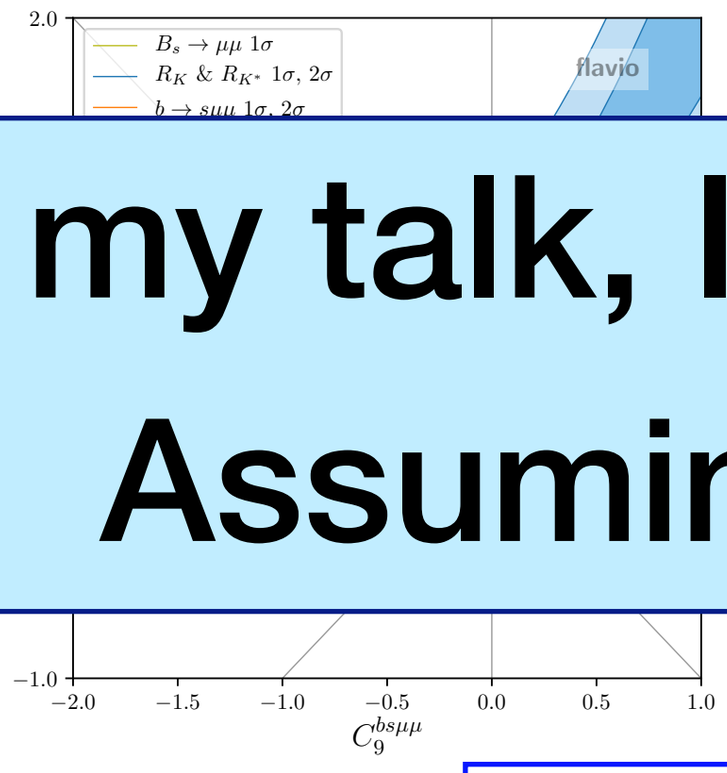

After Moriond 2021

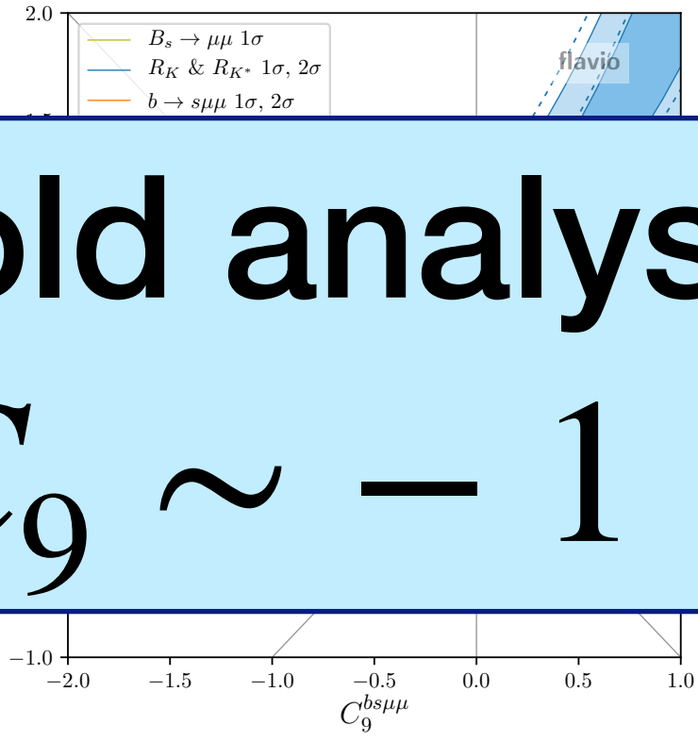

In my talk, I use old analysis, Assuming $\Delta C_9 \sim -1$

After Moriond 2021

- R_K **: smaller uncertainty**
- $B_s \to \mu\mu$ **: smaller uncertainty & better agreement with** $b \to s\mu\mu$

Simplest Extra Z' Models

He, Joshi, Lew, Volkas : PRD 43, R22 (1991), PRD44, 2118 (1991)

- Gauge anomaly free extensions of the SM without extra fermions : $U(1)_{e-\mu}$, $U(1)_{\mu-\tau}$, $U(1)_{\tau-e}$

- $U(1)_{B-L}$: Anomaly free with 3 RH neutrinos

- Generalization of $U(1)_{B-L}$: family dependent version, $U(1)_{B-\sum_i x_i L_i}$ (with $\sum x_i = 3$)

Muon (g-2) in $U(1)_{\mu-\tau}$ Model

Baek, Deshpande, He, Ko : hep-ph/0104141
Baek, Ko : arXiv:0811.1646 [hep-ph]

$$\begin{array}{ll} L_L^e: (1,2,-1)(0) & e_R: (1,1,-2)(0) \\ L_L^\mu: (1,2,-1)(2a) & \mu_R: (1,1,-2)(2a) \\ L_L^\tau: (1,2,-1)(-2a) & \mu_R: (1,1,-2)(-2a). \end{array}$$

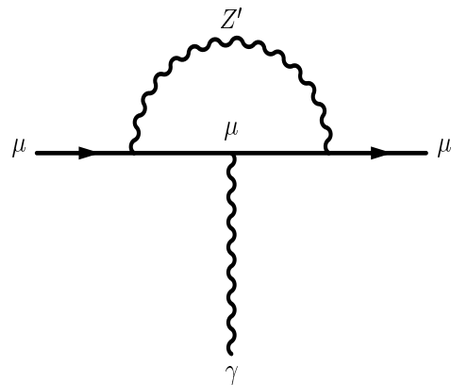

$$\Delta a_\mu = \frac{\alpha'}{2\pi}\int_0^1 dx \frac{2m_\mu^2 x^2(1-x)}{x^2 m_\mu^2 + (1-x)M_{Z'}^2} \approx \frac{\alpha'}{2\pi}\frac{2m_\mu^2}{3M_{Z'}^2}$$

$$Z' \to \mu^+\mu^-, \tau^+\tau^-, \nu_\alpha\bar{\nu}_\alpha \text{ (with } \alpha = \mu \text{ or } \tau), \ \psi_D\overline{\psi}_D$$

$\Gamma(Z' \to \mu^+\mu^-) = \Gamma(Z' \to \tau^+\tau^-) = 2\Gamma(Z' \to \nu_\mu\bar{\nu}_\mu) = 2\Gamma(Z' \to \nu_\tau\bar{\nu}_\tau) = \Gamma(Z' \to \psi_D\bar{\psi}_D)$

if $M_{Z'} \gg m_\mu, m_\tau, M_{\rm DM}$. The total decay rate of Z' is approximately given by

$$\Gamma_{\rm tot}(Z') = \frac{\alpha'}{3} M_{Z'} \times 4(3) \approx \frac{4(\text{or } 3)}{3} \text{ GeV} \left(\frac{\alpha'}{10^{-2}}\right) \left(\frac{M_{Z'}}{100\text{GeV}}\right)$$

$$\begin{aligned} q\bar{q} \text{ (or } e^+e^-) &\to \gamma^*, Z^* \to \mu^+\mu^- Z', \tau^+\tau^- Z' \\ &\to Z^* \to \nu_\mu\bar{\nu}_\mu Z', \nu_\tau\bar{\nu}_\tau Z' \end{aligned}$$

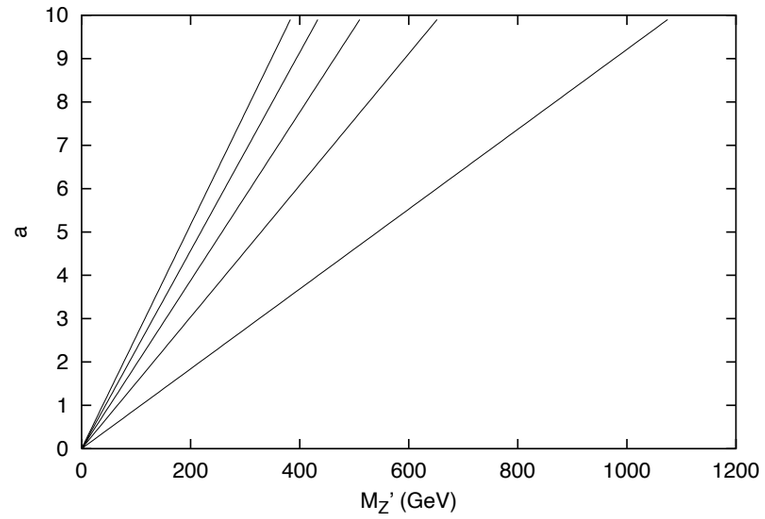

FIG. 2. Δa_μ on the a vs. $m_{Z'}$ plane in case b). The lines from left to right are for Δa_μ away from its central value at $+2\sigma, +1\sigma, 0, -1\sigma$ and -2σ, respectively.

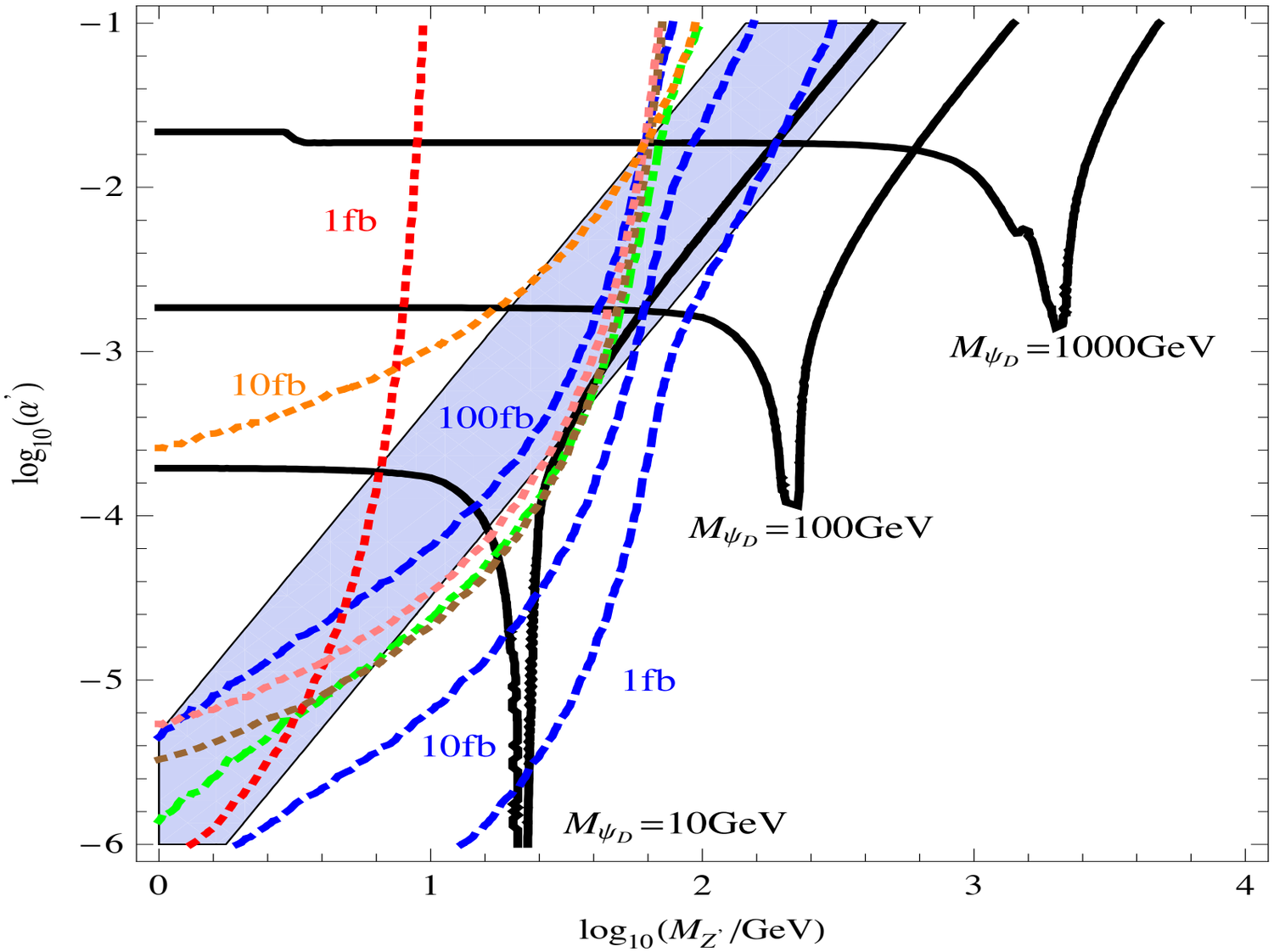

Figure 1: The relic density of CDM (black), the muon $(g-2)_\mu$ (blue band), the production cross section at B factories (1 fb, red dotted), Tevatron (10 fb, green dotdashed), LEP (10 fb, pink dotted), LEP2 (10 fb, orange dotted), LHC (1 fb, 10 fb, 100 fb, blue dashed) and the Z^0 decay width ($2.5\ \times 10^{-6}$ GeV, brown dotted) in the $(\log_{10}\alpha', \log_{10} M_{Z'})$ plane. For the relic density, we show three contours with $\Omega h^2 = 0.106$ for $M_{\psi_D} = 10$ GeV, 100 GeV and 1000 GeV. The blue band is allowed by $\Delta a_\mu = (302 \pm 88) \times 10^{-11}$ within 3 σ.

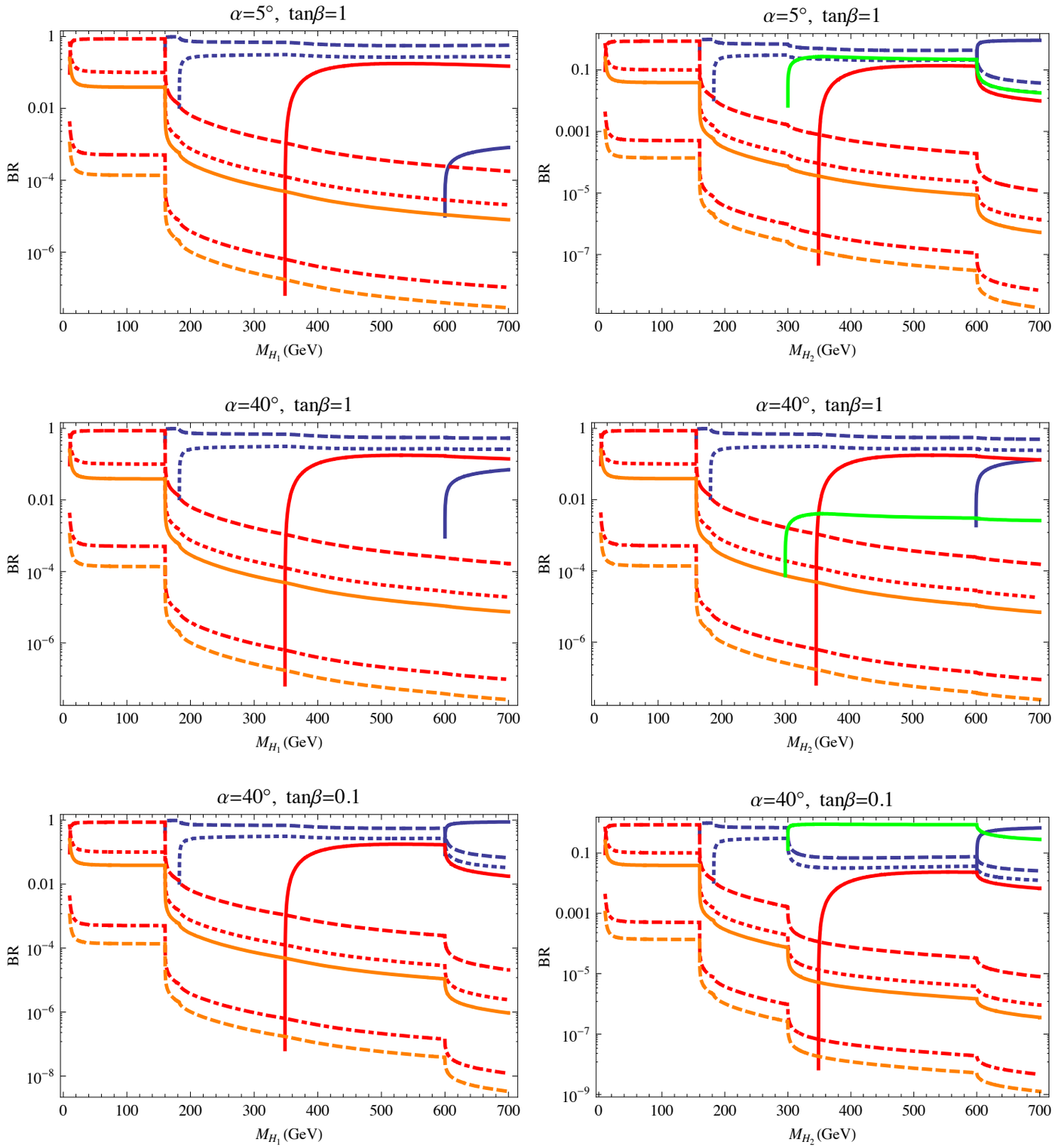

Figure 7: In the left (right) column are shown the branching ratios of the lighter (heavier) Higgs $H_{1(2)}$ into two particles in the final states: $t\bar{t}$ (solid in red), $b\bar{b}$ (dashed red), $c\bar{c}$ (dotted red), $s\bar{s}$ (dot-dashed red), $\tau\bar{\tau}$ (solid orange), $\mu\bar{\mu}$ (dashed orange), WW (dashed blue), ZZ (dotted blue) and $Z^{'}Z^{'}$ (solid blue) for difference values of the mixing angle α and $\tan\beta$. We fixed $M_{Z'} = 300$ GeV. We also fixed $M_{H_2} = 700$ GeV ($M_{H_1} = 150$ GeV) for the plots of the left (right) column.

$R(K^{(*)})$ in $U(1)_{\mu-\tau}$ Model

Ko, Okada, Nomura : arXiv:1702.02699 [hep-ph]

	Q'_a	χ
$SU(3)_C$	**3**	**1**
$SU(2)_L$	**2**	**1**
$U(1)_Y$	$\frac{1}{6}$	0
$U(1)_{\mu-\tau}$	q_x	q_x

TABLE I: Charge assignments of the new fields Q' and χ under $SU(3)_C \times SU(2)_L \times U(1)_Y \times U(1)_{\mu-\tau}$ with $q_x \neq 0$ where we assume these fields have Z_2 odd parity. Here Q' is vector-like fermions, and its lower index a is the number of family that runs over $1-3$. χ is a complex boson that is considered as a DM candidate.

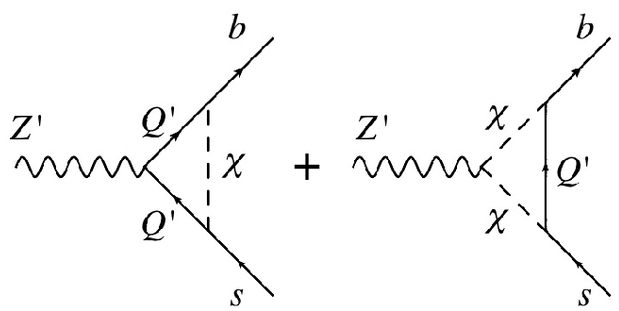

Assumed

$$\Delta C_9 \sim -1$$

(Pre Moriond 2021)

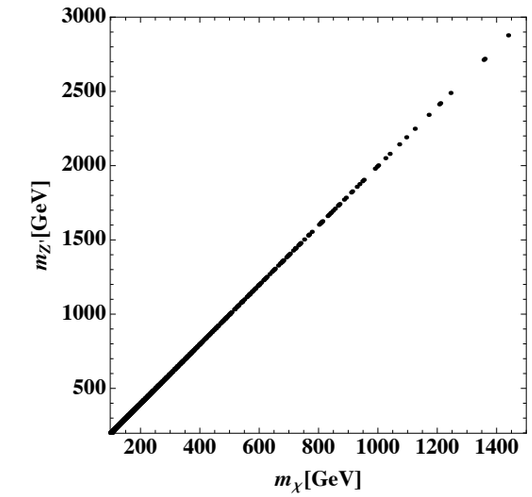

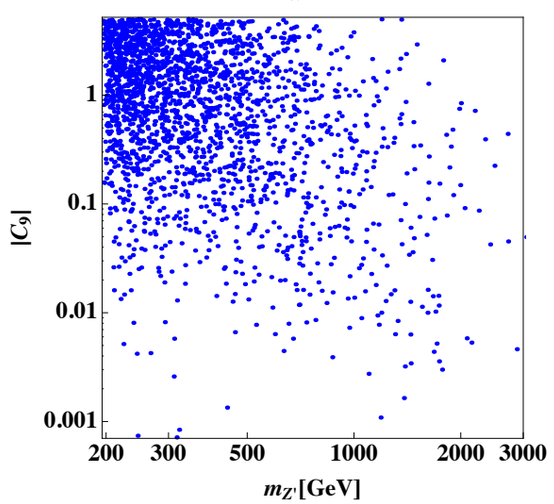

FIG. 2: The top panel represents the allowed range for m_χ and $m_{Z'}$, while the bottom one does the allowed range for $m_{Z'}$ and ΔC_9. The correlation between m_χ and $m_{Z'}$ in the top panel arises from the relation of relic density of DM. In the bottom panel, one finds that one can obtain $\Delta C_9 \sim -1$ for $m_{Z'} \lesssim 2$ TeV that is required to resolve $B \to K^{(*)}\ell^+\ell^-$ anomalies.

- Constraints : $M - \overline{M}$ mixing, $b \to s\gamma$, DM phenomenology, Collider searches for extra VLQ's

$R(K^{(*)})$ in $U(1)_{B_3-x_\mu L_\mu - x_\tau L_\tau}$ Model

Ko, Nomura, Yu : arXiv:1902.06107 [hep-ph]

Fermions	Q_{iL}	u_{iR}	d_{iR}	Q_{3L}	t_R	b_R	L_{1L}	L_{2L}	L_{3L}	e_R	μ_R	τ_R	ν_{1R}	ν_{2R}	ν_{3R}
$SU(3)_C$	**3**	**3**	**3**	**3**	**3**	**3**	**1**	**1**	**1**	**1**	**1**	**1**	**1**	**1**	**1**
$SU(2)_L$	**2**	**1**	**1**	**2**	**1**	**1**	**2**	**2**	**2**	**1**	**1**	**1**	**1**	**1**	**1**
$U(1)_Y$	$\frac{1}{6}$	$\frac{2}{3}$	$-\frac{1}{3}$	$\frac{1}{6}$	$\frac{2}{3}$	$-\frac{1}{3}$	$-\frac{1}{2}$	$-\frac{1}{2}$	$-\frac{1}{2}$	-1	-1	-1	0	0	0
$U(1)_X$	0	0	0	$\frac{1}{3}$	$\frac{1}{3}$	$\frac{1}{3}$	0	$-x_\mu$	$-x_\tau$	0	$-x_\mu$	$-x_\tau$	0	$-x_\mu$	$-x_\tau$

Table 1. Charge assignment for the SM fermions and right-handed neutrinos where the indices $i = 1, 2$ indicate the first and second generations.

$x_\mu + x_\tau = 1$ **for anomaly cancelaltion**

- Can discuss B physics, DM, neutrino physics, CLFV, etc..

Fields	Φ_1	Φ_2	φ_1	φ_2	χ
$SU(2)_L$	**2**	**2**	**1**	**1**	**1**
$U(1)_Y$	$\frac{1}{2}$	$\frac{1}{2}$	0	0	0
$U(1)_X$	$-\frac{1}{3}$	0	$\frac{1}{3}$	1	$\frac{5}{6}$

Table 2. Scalar fields and extra fermion χ in the minimal model and their representation under $SU(2) \times U(1)_Y \times U(1)_X$ where these fields are color singlet.

2HDM in this model

$$\Phi_1 \ : \ (\mathbf{1},\mathbf{2})(1/2,-1/3), \quad \Phi_2 \ : \ (\mathbf{1},\mathbf{2})(1/2,0), \quad (SU(3)_C, SU(2)_L)(U(1)_Y, U(1)_X)$$

Need 2HMD for a realistic Yukawa's for quarks and leptons

$$\begin{aligned} -\mathcal{L}_Q =& y^u_{ij}\bar{Q}_{iL}\tilde{\Phi}_2 u_{jR} + y^d_{ij}\bar{Q}_{iL}\Phi_2 d_{jR} + y^u_{33}\bar{Q}_{3L}\tilde{\Phi}_2 t_R + y^d_{33}\bar{Q}_{3L}\Phi_2 b_R \\ &+ \tilde{y}^u_{3i}\bar{Q}_{3L}\tilde{\Phi}_1 u_{iR} + \tilde{y}^d_{i3}\bar{Q}_{iL}\Phi_1 b_R + \text{h.c.}, \end{aligned}$$

$$M^u = \frac{1}{\sqrt{2}}\begin{pmatrix} v_2 y^u_{11} & v_2 y^u_{12} & 0 \\ v_2 y^u_{21} & v_2 y^u_{22} & 0 \\ 0 & 0 & v_2 y^u_{33} \end{pmatrix} + \begin{pmatrix} 0 & 0 & 0 \\ 0 & 0 & 0 \\ (\xi_u)_{31} & (\xi_u)_{32} & 0 \end{pmatrix}$$

$$M^d = \frac{1}{\sqrt{2}}\begin{pmatrix} v_2 y^d_{11} & v_2 y^d_{12} & 0 \\ v_2 y^d_{21} & v_2 y^d_{22} & 0 \\ 0 & 0 & v_2 y^d_{33} \end{pmatrix} + \begin{pmatrix} 0 & 0 & (\xi_d)_{13} \\ 0 & 0 & (\xi_d)_{23} \\ 0 & 0 & 0 \end{pmatrix}.$$

$$(\xi_{u,d})_{ij} \equiv \tilde{y}^{u,d}_{ij} v_1/\sqrt{2}$$

$R(K^{(*)})$ anomaly

$$\Delta C_9^\mu = \frac{x_\mu g_X^2}{3m_{Z'}^2}\left(\frac{\sqrt{2}\pi}{G_F\alpha_{em}}\right) \simeq 2.78 \times x_\mu \left(\frac{g_X}{0.62}\right)^2 \left(\frac{1.5\ \text{TeV}}{m_{Z'}}\right)^2 \sim -1$$

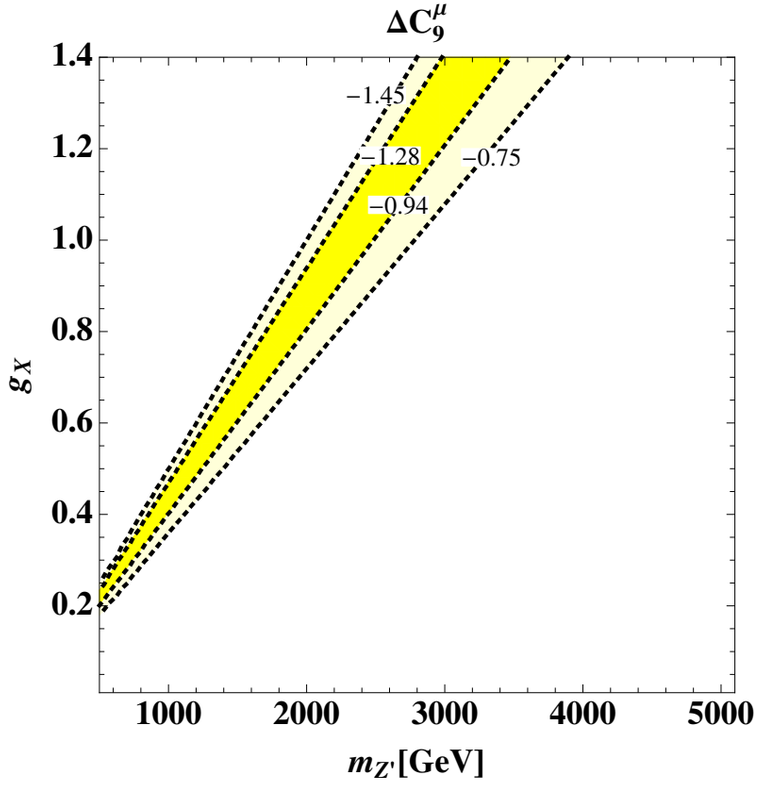

Figure 1. The contours showing Z' contribution to ΔC_9^μ on the $m_{Z'}$-g_X plane with $x_\mu = -\frac{1}{3}$ where yellow(light-yellow) region corresponds to 1σ (2σ) region from global fit in Ref. [11].

CLFV : $\mu \to e\gamma$

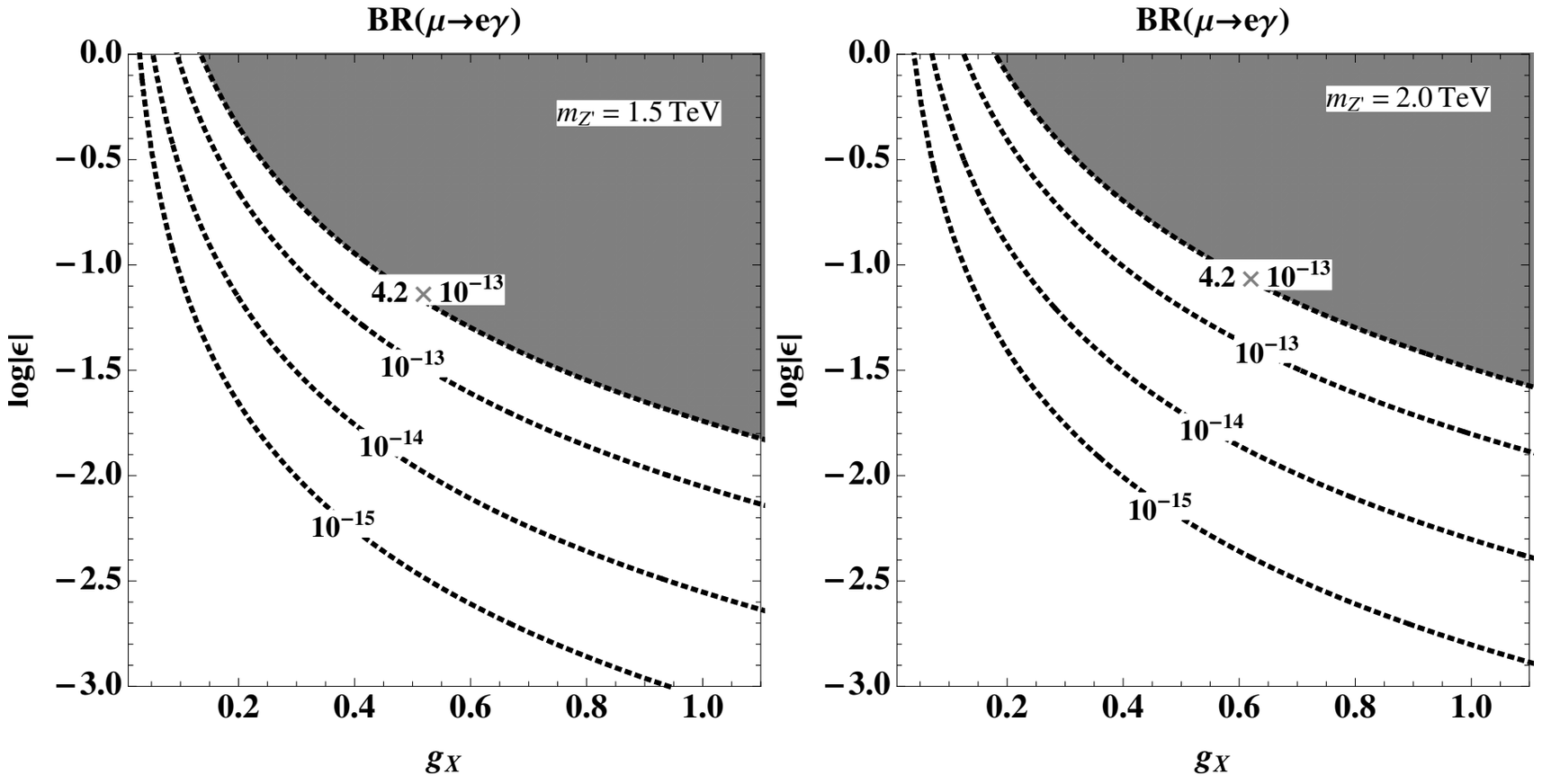

Figure 3. $BR(\mu \to e\gamma)$ as a function of $\{g_X, \log|\epsilon|\}$ fixing $m_{Z'} = 1.5(2.0)$ TeV for left(right) plot where the shaded regions are excluded.

$\mu \to e$ Conversion

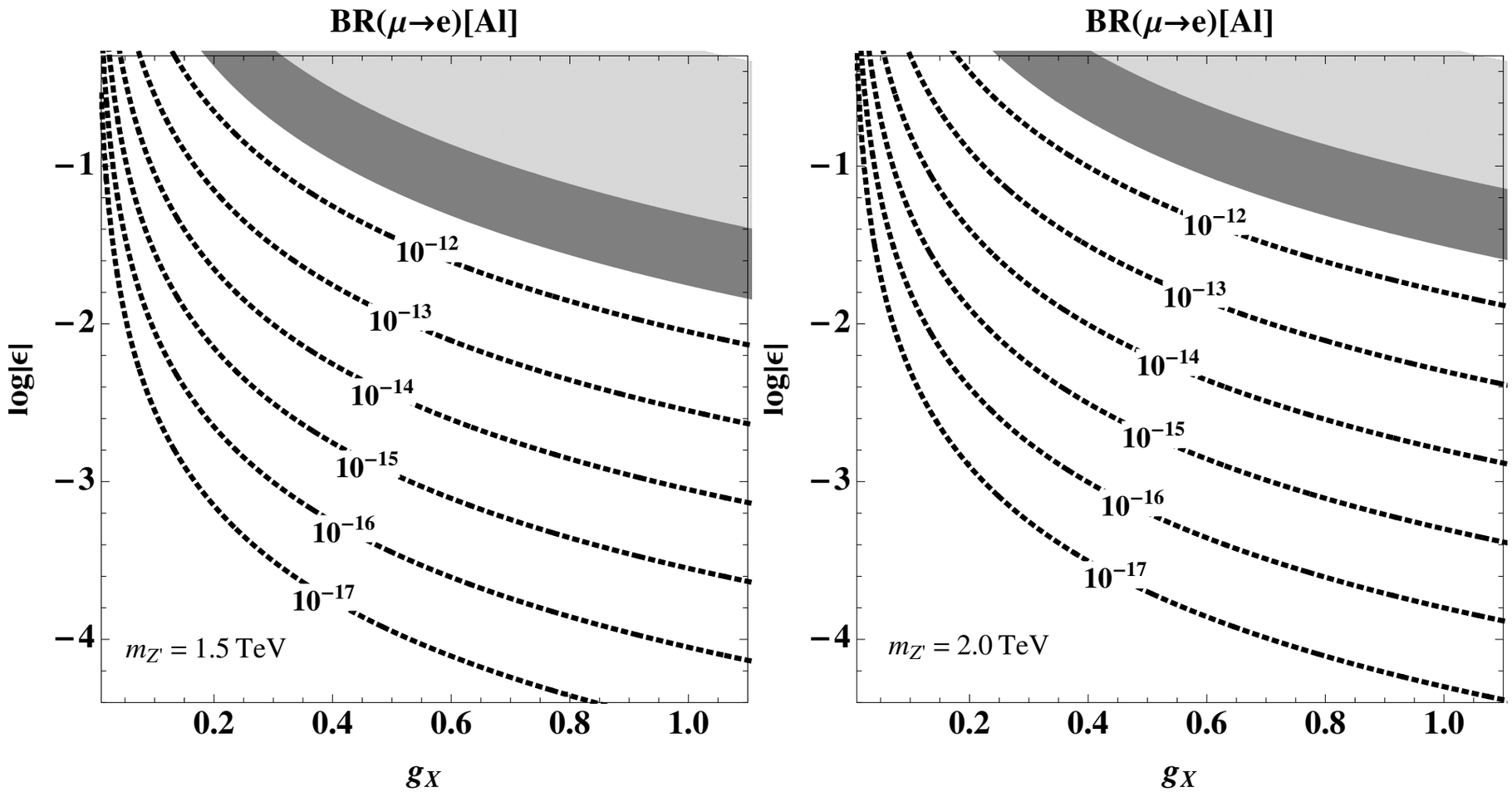

Figure 4. $BR(\mu \to e)$ on $^{27}_{13}$Al as a function of $\{g_X, \log|\epsilon|\}$ fixing $m_{Z'} = 1.5(2.0)$ TeV for left(right) plot where gray(light-gray) shaded region is excluded by current $\mu \to e\gamma$ BR ($\mu \to e$ BR on $^{197}_{79}$Au [55]) constraints.

$R(D^{(*)})$ vs. Top FCNC

TJKim, Ko, Li, JPark, Wu : arXiv:1812.08484 [hep-ph]

- Scalar LQ S_1 (3,1,1/3) and VLQ U_1^μ (3,1,2/3)

$$\begin{aligned}\mathcal{L}_{S_1} &= g_{1L}^{ij}\,\overline{Q_i^C}\,i\tau_2 L_j S_1 + g_{1R}^{ij}\,\overline{u_{Ri}^C}\,e_{Rj}S_1 + \text{h.c.},\\ \mathcal{L}_{U_1} &= h_{1L}^{ij}\,\overline{Q}_i\gamma_\mu L_j U_1^\mu + h_{1R}^{ij}\,\overline{d}_{Ri}\gamma_\mu \ell_{Rj} U_1^\mu + \text{h.c.},\end{aligned}$$

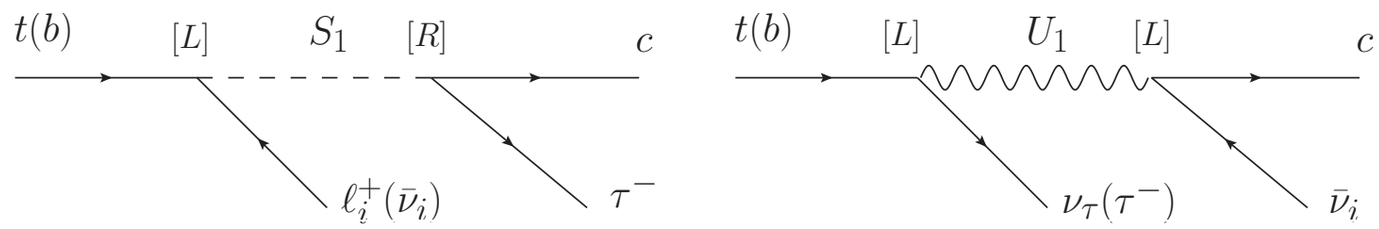

Figure 1: Tree-level top FCNC decays considered in this work, induced by SU(2) singlet scalar LQ S_1 and vector LQ U_1.

H_{eff} for $B \to D^{(*)} l\nu$

$$-\mathcal{L}_{\text{eff}} = (C_{\text{SM}}\delta_{l\tau} + C_{V_1}^l)O_{V_1}^l + C_{V_2}^l O_{V_2}^l + C_{S_1}^l O_{S_1}^l + C_{S_2}^l O_{S_2}^l + C_T^l O_T^l$$

$$\begin{aligned}
O_{V_1}^l &= (\bar{c}_L\gamma^\mu b_L)(\bar{\tau}_L\gamma_\mu\nu_{lL})\,, \quad & O_{V_2}^l &= (\bar{c}_R\gamma^\mu b_R)(\bar{\tau}_L\gamma_\mu\nu_{lL})\,, \\
O_{S_1}^l &= (\bar{c}_L b_R)(\bar{\tau}_R\nu_{lL})\,, & O_{S_2}^l &= (\bar{c}_R b_L)(\bar{\tau}_R\nu_{lL})\,, \\
O_T^l &= (\bar{c}_R\sigma^{\mu\nu} b_L)(\bar{\tau}_R\sigma_{\mu\nu}\nu_{lL})\,.
\end{aligned}$$

$$\begin{aligned}
C_{V_1}^l &= \sum_{k=1}^{3} V_{k3}\left(\frac{g_{1L}^{kl} g_{1L}^{23*}}{2M_{S_1}^2} + \frac{h_{1L}^{2l} h_{1L}^{k3*}}{M_{U_1}^2}\right)\,, \quad & C_{V_2}^l &= 0\,, \\
C_{S_1}^l &= \sum_{k=1}^{3} V_{k3}\left(-\frac{2h_{1L}^{2l} h_{1R}^{k3*}}{M_{U_1}^2}\right)\,, & C_{S_2}^l &= \sum_{k=1}^{3} V_{k3}\left(-\frac{g_{1L}^{kl} g_{1R}^{23*}}{2M_{S_1}^2}\right) \\
C_T^l &= \sum_{k=1}^{3} V_{k3}\left(\frac{g_{1L}^{kl} g_{1R}^{23*}}{8M_{S_1}^2}\right)\,.
\end{aligned}$$

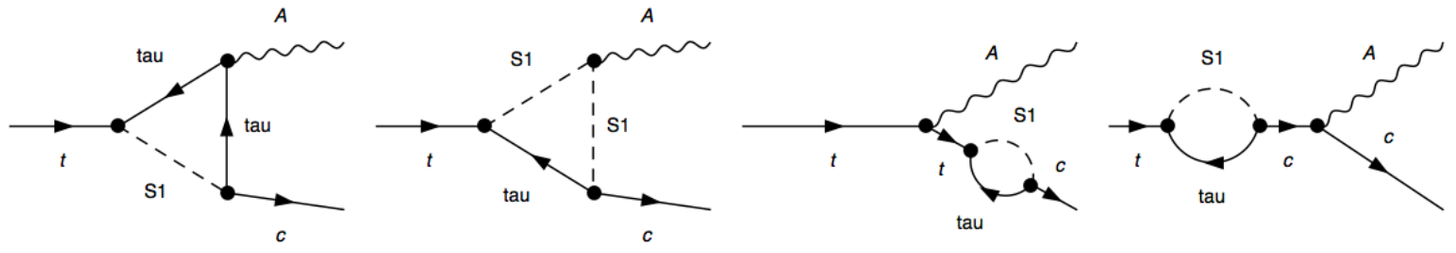

Figure 2: One-loop top FCNC decays of $t \to c\gamma$ considered in this work, induced by SU(2) singlet scalar LQ S_1.

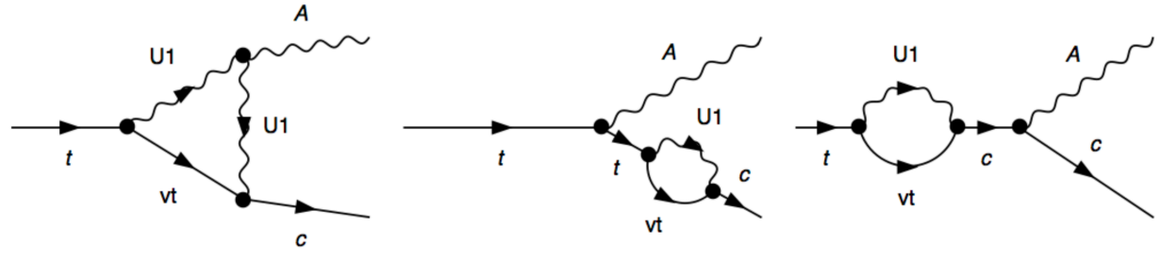

Figure 3: One-loop top FCNC decays of $t \to c\gamma$ induced by SU(2) singlet vector LQ U_1. Note that we do not calculate these diagrams in this work, due to the lack of ultraviolet completion for vector LQ U_1 in our phenomenological studies. See more discussions in Section 3.2.

LQ	2σ range for $\bar{B} \to D^{(*)}\tau\bar{\nu}$	
S_1	$g_{1L}^{3l} g_{1R}^{23*} \in \left(\frac{M_{S_1}}{1\text{ TeV}}\right)^2 \times$	$(1.64, 1.81)$ $\quad l = 1, 2$ $(-0.87, -0.54)$ $\quad l = 3$
U_1	$h_{1L}^{2l} h_{1L}^{33*} \in \left(\frac{M_{U_1}}{1\text{ TeV}}\right)^2 \times$	$(0.52, 0.84)$ $\quad l = 1, 2$ $(-2.94, -2.80)$ $\quad l = 3$

Predictions for Top FCNC

$$S_1 : Br(t \to c\tau^- \ell_l^+) \approx \frac{1}{\Gamma_{t,SM}} \Big(\frac{m_t^5}{6144\pi^3} \Big) |\frac{g_{1L}^{3l} g_{1R}^{23*}}{M_{S_1}^2}|^2 = 10^{-6} \times \begin{cases} 1.4 \sim 1.8 & l = 1,2 \\ 0.16 \sim 0.41 & l = 3 \end{cases} \quad (3.1)$$

$$U_1 : Br(t \to c\nu_\tau \bar{\nu}_l) \approx \frac{1}{\Gamma_{t,SM}} \Big(\frac{m_t^5}{1536\pi^3} \Big) |\frac{h_{1L}^{33} h_{1L}^{2l*}}{M_{U_1}^2}|^2 = 10^{-6} \times \begin{cases} 0.58 \sim 1.5 & l = 1,2 \\ 17 \sim 19 & l = 3 \end{cases} \quad (3.2)$$

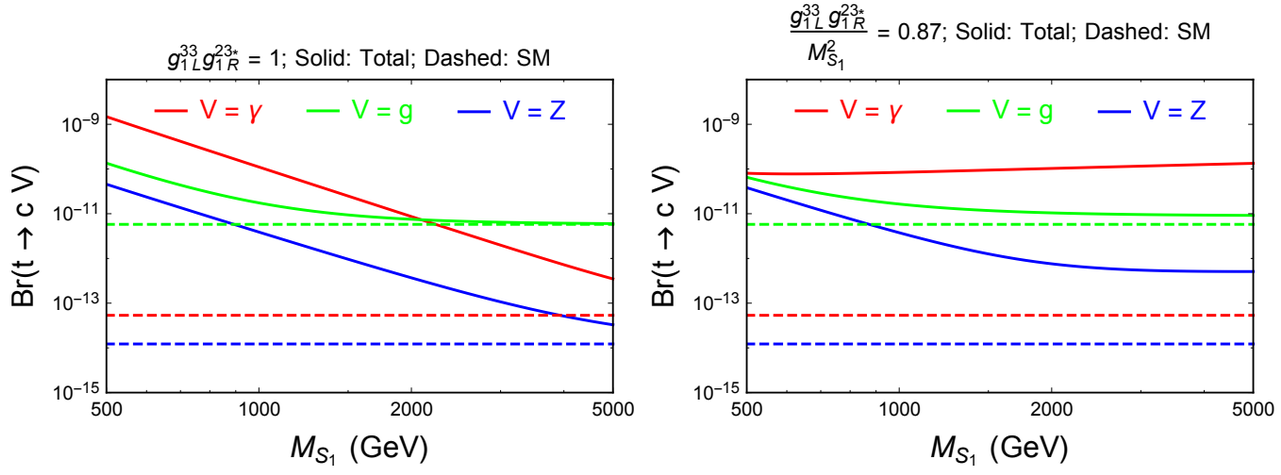

Figure 4: $Br(t \to cV)$, $V = \gamma, g, Z$ at one-loop level induced by SU(2) singlet scalar LQ S_1. In the left panel we choose $g_{1L}^{33} g_{1R}^{23*} = 1$ as an ordinary coupling benchmark to show the decoupling behavior of LQ S_1 contribution with respect to M_{S_1}. In the right panel, we fix $\frac{g_{1L}^{33} g_{1R}^{23*}}{M_{S_1}^2} = 0.87$ which is the upper bound value of numerical fitting for LQ models to explain $R_{D^{(*)}}$ at 2σ (see Table.1). Solid lines include both the SM and the LQ contribution, while dashed lines are the SM predictions with the CKM matrix values taken from Particle Data Group [138].

Conclusions

- A number of anomalies in the low energy physics : muon, B physics, Cabbibo angle, ….

- Some anomalies (~2σ-ish) at LHC (@KFCC, KITP workshop)

- Need more data accumulations and improvement of theory predictions

- Cross check a solution in various channels (B vs. top, e.g.)

- Many possibilities for each or a few anomalies [except for $R^{(*)}(D)$ anomaly]

- Can we have a consistent UV complete model that can account for flavor anomalies and/or collider anomalies ?